To cite this version :

Sébastien DUBENT, Alexandra MAZARD - Characterization and corrosion behaviour of grade 2 titanium used in electrolyzers for hydrogen production - International Journal of Hydrogen Energy - Vol. 44, n°29, p.15622-15633 - 2019

Characterization and corrosion behaviour of grade 2 titanium used in electrolyzers for hydrogen production

Sébastien Dubent [a],[*], Alexandra Mazard [b]

[a] *Laboratoire PIMM (Propriétés Ingénierie Mécanique et Matériaux), UMR CNAM ENSAM CNRS 8006, Conservatoire National des Arts et Métiers (CNAM), EPN 04 - 2, rue Conté, 75003 Paris, France*

[b] *Laboratoire de Matériaux Industriels Métalliques et Polymères, Conservatoire National des Arts et Métiers (CNAM), EPN 04 - 2, rue Conté, 75003 Paris, France*

Keywords:
Titanium
Electrolyzers
Characterization
Corrosion
Hydrogen
GDOES

ABSTRACT

The decentralized production of hydrogen as a renewable energy vector targets large markets and potential applications: mobility, electricity and fixed heat generation, electricity storage in the form of gas. Hydrogen is today in France and in the industrialized countries an emerging industrial sector, leading to an increasing development of electrolyzers. The study of the behaviour of grade 2 titanium used in these electrolyzers for hydrogen production, using a characterization of parts by Scanning Electron Microscopy (SEM), surface analysis by Glow Discharge Optical Emission Spectrometry (GDOES) demonstrating the hydrogen diffusion in titanium, and electrochemical measurements, will make it possible to understand and interpret the mechanisms that caused degradation after 5000 h of operation and to validate the choice of grade 2 titanium.

Contents

---

* *Corresponding author.*
  E-mail addresses: sebastien.dubent@lecnam.net, sebastien.dubent@ensam.eu (S. Dubent).

Introduction

The rapid depletion of energy resources, fossil energies being non-renewable, added to the growing environmental problems, have led to urgent need for clean and sustainable energy sources [1–4]. Hydrogen is a promising alternative today because of its environment benignity and high gravity energy density [5–7]. Hydrogen hardly exists in its natural state. More than 95% of the world's hydrogen is still produced by steam reforming hydrocarbons, particularly natural gas, a process for dissociating carbon molecules in the presence of water vapour and heat. Alongside this production route, in response to the imperatives of the fight against climate change, processes are developing, using renewable primary sources (renewable electricity, solid biomass, biogas) to synthesize hydrogen, which we describe as therefore renewable [8]. Among them, electrolysis of water offers an easy method for cleanliness and safety hydrogen production [9–11]. This electrochemical process produce hydrogen and oxygen from water, in electrolyzers, whose electrodes and gas storage tanks (gas/liquid separators), as part of this study, are grade 2 titanium. It should be noted that the choice to use titanium for the hydrogen/liquid separator, even if it is not common in electrolyzers because of its high cost, is a strategic choice of our industrial partner in order to increase component durability.

The hydrogen thus produced can be used as an electricity storage solution, an interesting solution in the case of intermittent renewable electricity generation. The electricity is then transformed into hydrogen by electrolysis of water, which is then recovered as a fuel gas or converted back into electricity by a fuel cell in mobile or stationary applications.

The emergence of these renewable production routes and these applications implies a more decentralized mode of production than is currently the case in industry, particularly because the resources (water, renewable electricity, biogas and biomass) will be mainly available in the local scale and that uses (service stations or domestic use) will be decentralized. Electrolysis of water and steam reforming of biogas are currently the closest decentralized and renewable hydrogen production routes to the market in France for mobility, energy storage and energy supply applications of isolated sites. A number of French companies are developing these technologies, and many pilot or demonstration projects are underway at a more or less advanced level of development [12]. This study, aimed at characterizing the corrosion resistance of titanium used in the design of electrolyzers for hydrogen production, fits perfectly within this framework and is therefore of particular interest.

In addition, just like other combustible gases or energy sources, handling hydrogen involves risks. The peculiarities of hydrogen, compared to other fuels such as natural gas or gasoline, have imposed new know-how and new practices to ensure the safety of exposed people. In France, the regulatory framework for decentralized hydrogen production facilities is that of texts designed for larger-scale hydrogen production. It is therefore necessary today to ensure the resistance of all materials used in the design of these facilities, materials of which titanium is now a part, to capitalize knowledge and methods of risk control, and to disseminate them to the actors who will intervene in the development of the hydrogen-energy sector.

Titanium is widely used in the aerospace, automotive, chemical, and biomedical industries for its excellent corrosion resistance, bio-compatibility, high specific strength and low density [13–15]. Many studies have shown that the excellent corrosion resistance of titanium is mainly due to the presence of a very stable oxide film (TiO$_2$) on its surface [16–18]. Although this oxide film is very thin, it is a barrier to protect the metal in a corrosive environment. In addition, when the film is destroyed, it tends to reform very quickly in response to the aggressiveness of the environment. Indeed, the corrosion resistance property of titanium does not come from its resistance to oxidation, as for noble metals such as gold or platinum. Titanium is a very reactive metal that oxidizes spontaneously. The formed oxide layer becomes very protective and tight and its thickness increases slowly. Titanium resists well in acidic environments, except when the pH becomes too low, and it also resists in oxidizing media. The International Committee on Industrial Chimneys (ICIC), for example, recommends the use of pure titanium as an insertion material in the design of the chimney of coal-fired power plants, which means that pure titanium can resist in a strongly acidic medium (mixture of sulfuric acid, nitric acid and hydrochloric acid). However, it does not resist corrosion in the presence of fluoride ions and in very reducing media.

Finally, the welds are as strong as the base metal and the moulded parts are not a problem, as are the machining and shaping by plastic deformation.

Water electrolyzers for hydrogen production

A water electrolyzer is the simplest as the conversion device from renewable energy into hydrogen. Two major

technologies currently in use for water electrolyzers are alkaline electrolysis and proton exchange membrane (PEM) electrolysis [19,20].

In large scale industrial applications, alkaline electrolysis using liquid electrolyte consisting of 20−30 wt% potassium hydroxide (KOH) solution is dominant. Indeed it is the mature technology but, because hydrogen produced by an alkaline electrolyzer is derived with strong alkaline solution from the stacks, the balance of plant for the hydrogen purification process is complex and not suitable for buffering an intermittent power supply.

In contrast, PEM electrolysis is suitable for intermittent power input, and also capable of operation at higher current density (greater than 3 A/cm^2). PEM water electrolysis technology is frequently presented in the literature as a potentially very effective alternative to more conventional alkaline water electrolysis. PEM electrolysis systems offer several advantages over traditional technologies, including higher energy efficiency, higher production rates and more compact design. At given current density, PEM electrolysers have higher stack efficiencies than alkaline systems. However, a major drawback of PEM electrolysis is its high capital cost per power input and the acidic medium of the PEM technology limits the type of material that can be used for cell components to titanium.

These technical advantages of PEM electrolysis over alkaline electrolysis are mainly attributed to the membrane potential and cell structure. High proton conductivity and high mechanical/chemical stability of the proton exchange membrane technology enables stable electrolysis up to high current density (3−5 A/cm^2) [21].

PEM electrolysers technology

Electrolyzers studied, similar in design to PEM technology [22,23], mainly consist of a stack grouping a set of electrolytic cells for hydrogen production capacities ranging from 10 to 120 Nm^3/h. The hydrogen production capacity of a stack depends on the number of electrolytic cells composing it. For reasons of confidentiality, all the technology and the specific design of the stacks will not be developed in this article.

An electrolytic cell consists of two grade 2 titanium electrodes, separated by an ion exchange membrane, made from ceramic materials, the electrolyte being an aqueous solution of sulfuric acid (H$_2$SO$_4$ 1 M). These electrodes are connected to the opposite poles of a DC source. The H$_2$SO$_4$ molecule dissociates in water into sulphate (SO$_4^{2-}$) and hydrogen (2H$^+$) ions. In the cell, the hydrogen ions accept electrons at the cathode to form gaseous hydrogen (H$_2$), depending on the reduction reaction (1) [24]:

$$2H^+ + 2\,e^- \rightarrow H_2 \tag{1}$$

While an oxidation reaction of water occurs at the anode according to the reaction (2):

$$H_2O \rightarrow \tfrac{1}{2}\,O_2 + 2H^+ + 2\,e^- \tag{2}$$

The equation of decomposition by electrolysis of water, generating the production of oxygen and hydrogen, can therefore be written as follows (3):

$$H_2O_{(l)} \rightarrow H_{2(g)} + \tfrac{1}{2}\,O_{2(g)} \tag{3}$$

This decomposition requires a supply of electrical energy depending essentially on enthalpy and reaction entropy. The typical values of industrial cell potentials are of the order of 1.7−2.1 V [25−27].

The electrolysis power P is defined by (4):

$$P = U_{cell} \times I \tag{4}$$

where I is the current and U_{cell} the electrolysis voltage of the cell. The molar flow rate of hydrogen Δn is given by Faraday's law (5):

$$\Delta n = \frac{I}{n\,F} \tag{5}$$

where F is the Faraday constant and n the number of electrons exchanged during the reaction.

The dihydrogen (H$_2$) and dioxygen (O$_2$) produced (equation (3)) are recovered in titanium tanks (gas/liquid separators) through hoses in which the electrolyte circulates (Fig. 1). The titanium used to develop the electrodes and the tanks is a grade 2 titanium. The crystallographic structure of grade 2 titanium at a temperature below 882 °C (phase α) is hexagonal pseudo compact. Above this temperature, the structure is cubic centred (phase β) [28].

Definition of the study

Significant degradations on different parts of the electrolyzers, namely the hydrogen/H$_2$SO$_4$ separator (hydrogen recovery tank), the first electrodes input and output stacks, the cathodes of the electrolytic cells, could be observed after several hours of operation.

All these parts, grade 2 titanium, must be able to withstand the conditions proposed in the electrolyzers: temperature conditions (up to 60 °C), pressure (up to 16 bar) and medium of use (H$_2$SO$_4$ 1 M).

Indeed, although titanium is a chemically very reactive species, it is extremely oxidizable and, thanks to the formation on the surface of a protective oxide layer of a few
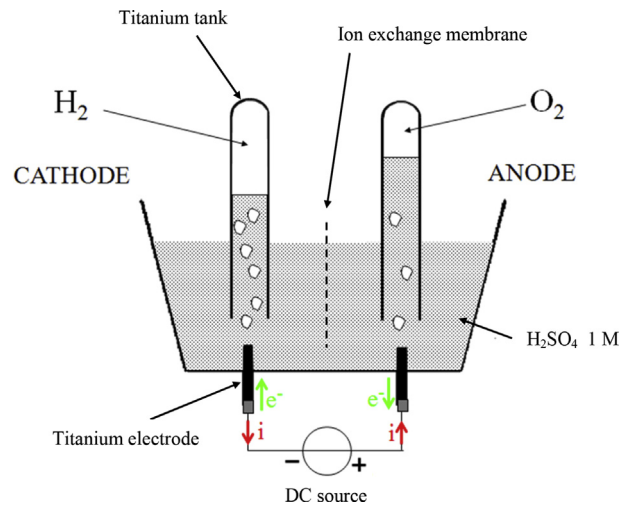

Fig. 1 − Operating principle of an electrolytic cell.

nanometres thick, is deemed to have a high corrosion resistance. This very adherent natural oxide layer reforms spontaneously if scratching of the surface in the presence of air or water [29]. However, very reductive conditions, as in concentrated sulfuric medium, decrease the protective nature of the layer and can cause corrosion. Therefore, in the case of the use of titanium in the design of electrolyzers for hydrogen production, the risk of degradation of parts is real. In addition, the presence of hydrogen in the system increases this risk and can exacerbate damage. Generally, hydrogen exerts a significant influence on almost all types of metallic materials, and titanium is no exception [30–32]. Many titanium equipment is still attacked in operation by hydrogen, because they may be in cathodic polarization condition or exposed to environments that can serve as sources of hydrogen. As a result, hydrogen can still diffuse into the surface oxide film until it contacts the titanium substrate, which can result in the formation of surface hydrides. The titanium dihydride (TiH_2) formed can notably induce radical changes in the properties of the film [33]. In addition, even small concentrations of hydrogen, not necessarily sufficient to form titanium hydrides, can also lead to failure after diffusion of hydrogen into the metal [34]. And if the solubility limit of hydrogen in titanium is reached, there may also be a precipitation of hydrides resulting in embrittlement. Hydrogen can distinctly alter the composition and adversely affect the performance of the oxide film and titanium, which can introduce uncertainties in the use of titanium in the design of electrolyzers for hydrogen production. It is therefore appropriate in this study to verify it and characterize more widely the corrosion resistance of titanium in sulfuric medium. These two phenomena, corrosion and hydrogenation, can cause a decrease in the lifetime and efficiency of electrolyzers, hence the need to determine the exact origin and to characterize the nature of the damage.

Material and methods

The work performed at the *Metallic Industrial Materials Laboratory of the Conservatoire National des Arts et Métiers (CNAM)* in Paris (France), was to characterize morphology of damage and determine corrosion mechanisms using Scanning Electron Microscopy (SEM), analyse, by Glow Discharge Optical Emission Spectrometry (GDOES), the possible embrittlement of titanium by hydrogen, and study the corrosion behaviour of grade 2 titanium using electrochemical methods, in the closest possible conditions on the operating conditions of an electrolyzer [35].

Scanning Electron Microscopy (SEM)

Many samples of degraded areas of grade 2 titanium parts were taken, respectively from the hydrogen/H_2SO_4 separator and electrodes of the stacks, after 5000 h of operation, at a temperature between 30 and 50 °C, a pressure up to 16 bar and a current of 0.3 A/dm^2 running through the electrolyte (H_2SO_4 1 M). SEM observations of these areas were performed using a Carl Zeiss EVO MA10 microscope to characterize the morphology of the degradations of titanium parts.

Glow Discharge Spectrometry (GDOES)

GDOES is a surface analytical technique, an atomic emission spectrometer system employing a non-thermal glow discharge source for atomic excitation [36]. In a glow discharge, cathodic sputtering is used to remove material layer by layer from the sample surface. The atoms removed migrate into the plasma where they are excited through collisions with electrons or metastable carrier gas atoms. The characteristic spectrum emitted by these excited atoms is measured by the optical spectrometer [37].

GDOES was used to characterize the possible embrittlement of titanium by hydrogen and to determine the diffusion depth of hydrogen in degraded areas of grade 2 titanium parts after 5000 h of operation.

The distribution of elements was determined qualitatively by depth profiling using a Horiba JY 10000 RF spectrometer equipped with a 4 mm diameter anode. The power to the plasma was supplied by a radio-frequency generator at a frequency of 13.56 MHz. A moderate power of 35 W was used for all analyses. High-purity argon was employed as the discharge gas, at a constant pressure of 650 Pa. The following atomic emission lines (H: 121.574 nm, O: 130.223 nm, C: 156.149 nm, S: 180.738 nm, Ti: 365.355 nm) were selected.

Resolution degradation occurred with increasing depth caused by non-uniform sputter erosion resulting in a deformed crater shape [38]. To counteract this inherent feature and to obtain optimum interface resolution, different discharge parameters were studied. The crater shape sputtered with the chosen parameters is relatively clean: the crater bottom is sufficiently flat and, the bottom and the surface roughness similar (Fig. 2).

The roughness profile of each crater then makes it possible to measure the eroded depth during the analysis, to deduce the sputtering rate and thus to calculate the thickness of the layers as well as the depth of diffusion of the hydrogen in each sample analysed.

Electrochemical measurements

The open-circuit potential (OCP) measurements as well as the potentiodynamic polarization curves are generally used to characterize corrosion behaviour of metallic materials [39–41]. Given this fact, we investigated the corrosion behaviour of grade 2 titanium using those electrochemical methods:
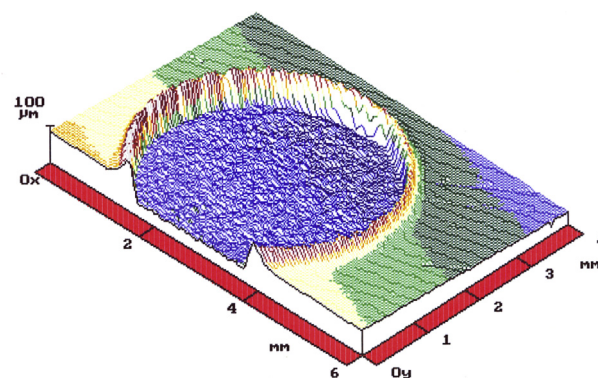

Fig. 2 – GDOES crater profile in a grade 2 titanium plate.

i.e. OCP and polarization curves to determine the corrosion currents (i_{corr}) by Tafel slopes [42].

All electrochemical measurements were performed at room temperature in a cell corrosion in sulfuric acid medium (H_2SO_4 1 M). A saturated calomel electrode (SCE) with a KNO_3 extension was used as the reference and a platinum sheet was employed as the counter electrode. The exposed surface of the working electrode, a sample of a grade 2 titanium plate, was 1 cm^2 (Fig. 3). A Radiometer Analytical PGZ 100 potentiostat under computer control was used as the electrochemical analyser system. The OCP of various grade 2 titanium samples were measured for about 24 h (1440 min) when they were immersed into the sulfuric acid solution. The polarization curves were recorded in a potential range from − 800 mV/SCE to + 1200 mV/SCE with a scanning rate of 1 mV/s and the corrosion currents were deduced from the Tafel slopes. Then, the corrosion rate of titanium in the medium was determined from Faraday's law (6):

$$m = \frac{1}{F}\frac{M}{n}\ i_{corr}\ t \text{ knowing that m} = \rho Se \qquad (6)$$

with m the corroded titanium mass, M and n respectively the molar mass and the valence of grade 2 titanium, F the Faraday constant, t the immersion time of the sample, ρ the grade 2 titanium density, S the surface of the sample and e the corroded thickness, which was calculated for a one-year immersion time [43].

Results and discussion

Corrosion morphology

SEM observations of degraded areas of grade 2 titanium parts, respectively taken from the hydrogen/H_2SO_4 separator and electrodes of the stacks, after 5000 h of operation of the electrolyzer, were performed.

Degradation of the hydrogen/H_2SO_4 separator

The first degraded part corresponds to the hydrogen/H_2SO_4 separator. This grade 2 titanium tank, electrically connected to the ground to avoid stray currents, contains the electrolyte (H_2SO_4 1 M) in the lower part and the hydrogen produced as well as vapours of sulfuric acid in the upper part (Fig. 4). To observe this tank, having a significant degradation, samples were taken from the lid.
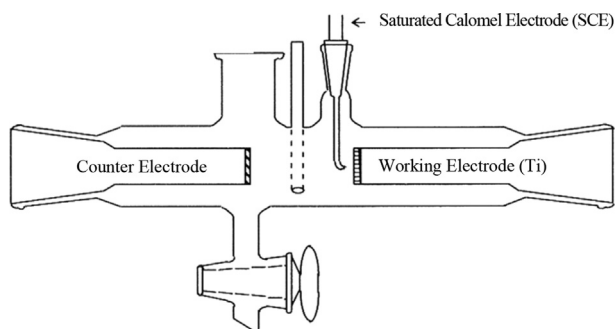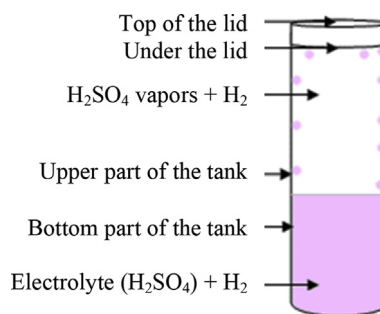

Fig. 3 − Corrosion cell.

Fig. 4 − Diagram of the hydrogen/H_2SO_4 separator.

The SEM observations of the underside of the tank lid, a particularly degraded area directly in contact with hydrogen gas and sulfuric acid vapours, reveal at low magnification an intergranular fracture on the surface (Fig. 5). This type of fracture, characteristic of the embrittlement at grain boundaries of a metallic material after hydrogen absorption [44,45], is particularly detrimental to the mechanical strength of the part, the embrittlement causing a grain boundaries decohesion and consequently a decrease in the mechanical properties of the material. Indeed, when the atomic hydrogen (H) diffuses into the titanium, the inclusions and impurities can allow to initiate its recombination in its diatomic form (H_2), thus generating very high pressures and causing the internal rupture of the material observed on the small-scale micrograph (Fig. 5).

Other SEM micrographs under greater magnification, still from the bottom of the tank lid, allow to highlight the presence of a very strongly degraded deposit on the surface of the titanium, the deposit having in fact significant cracks (Fig. 5). This deposit probably corresponds to a titanium oxide layer, covering itself, following the absorption of hydrogen, a hydride layer. The Glow Discharge Spectrometry (GDOES) analyses carried out during this study make it possible to verify this hypothesis.

In a second step, in order to characterize the depth of degradation of the underside of the titanium lid, a micrographic section of the degraded zone was also performed. The SEM observation of the section makes it possible to estimate the average depth of degradation of titanium at about 192 μm, which seems relatively important, even if the conditions of use are very severe (temperature between 30 and 50 °C, hydrogen pressure up to 16 bar and H_2SO_4 vapours), for an operating time of 5000 h, less than a year (Fig. 6).

To best characterize the degradation of the underside of the tank lid, SEM observations from the top of the lid, in contact with ambient air during the operation of the electrolyzer, were also performed. The images obtained reveal, at high magnification, only a very slightly degraded surface (Fig. 7). In addition, the absence of intergranular rupture confirms the role of hydrogen in the degradation of the surface of the underside of the tank lid.

Degradation of the electrodes

The SEM micrographs of the central zone of the electrodes, coated with Kynar® to protect titanium (not directly exposed
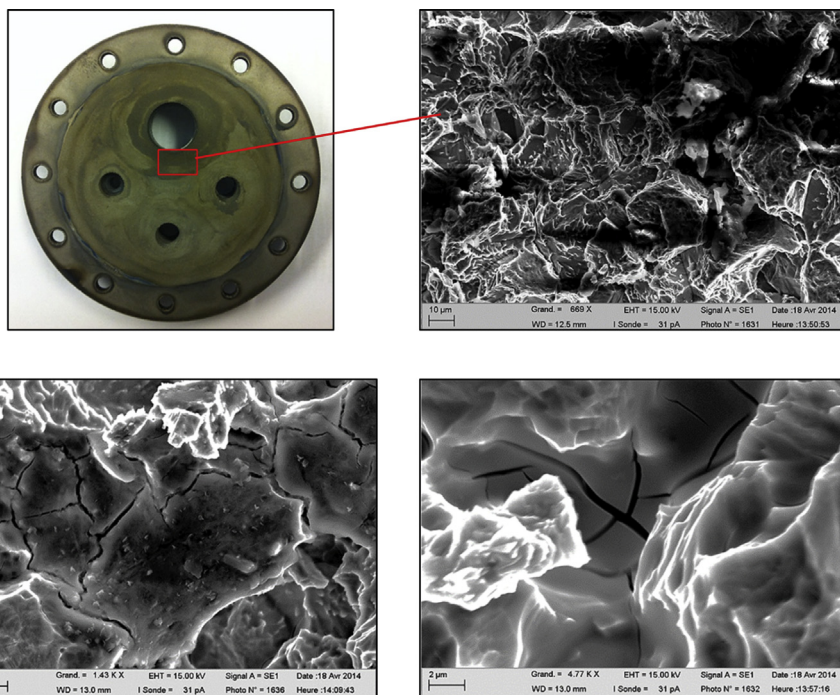
Fig. 5 – SEM micrographs of a degraded area of the grade 2 titanium hydrogen/H₂SO₄ separator (underside of the tank lid) after 5000 h of operation.
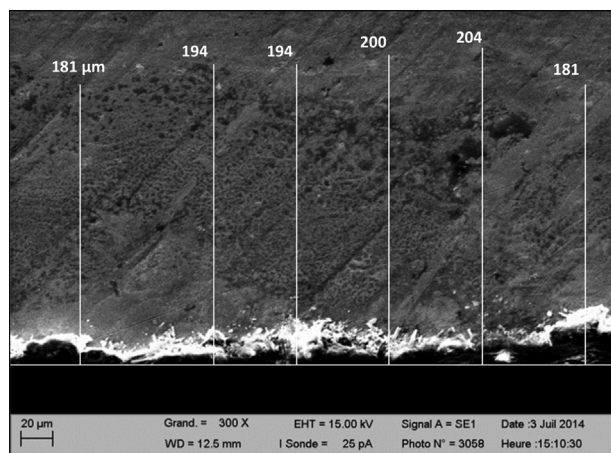

Fig. 6 – Micrographic section of the degraded zone of the underside grade 2 titanium lid after 5000 h of operation.

to sulfuric acid) and reduce contact resistance, do not allow to observe a real degradation, in accordance with the expectations related to the design of the stack. They reveal a granular structure and a slight natural porosity between the grains of titanium, according to the design of the electrodes (Fig. 8a1 and a2).

However, the characterization of an area at the edge of the electrodes, uncoated, reveals a significant degradation and, in addition to natural intergranular porosity, a high porosity in the grains themselves, mainly due to grain corrosion in sulfuric medium (Fig. 8b1). Many studies have been conducted to understand the mechanism of corrosion of titanium in sulfuric medium. It is generally accepted that the corrosion resistance of titanium can be destroyed by chemical dissolution of the protective oxide film, thus exposing the new titanium surface. Nevertheless, most studies have obtained this mechanism under the condition of anodic polarization by various electrochemical and surface analysis techniques
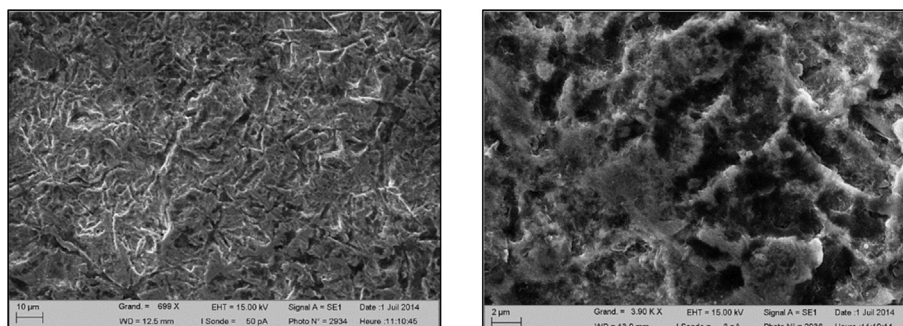

Fig. 7 – SEM micrographs of the grade 2 titanium hydrogen/H₂SO₄ separator. (top of the tank lid) after 5000 h of operation.
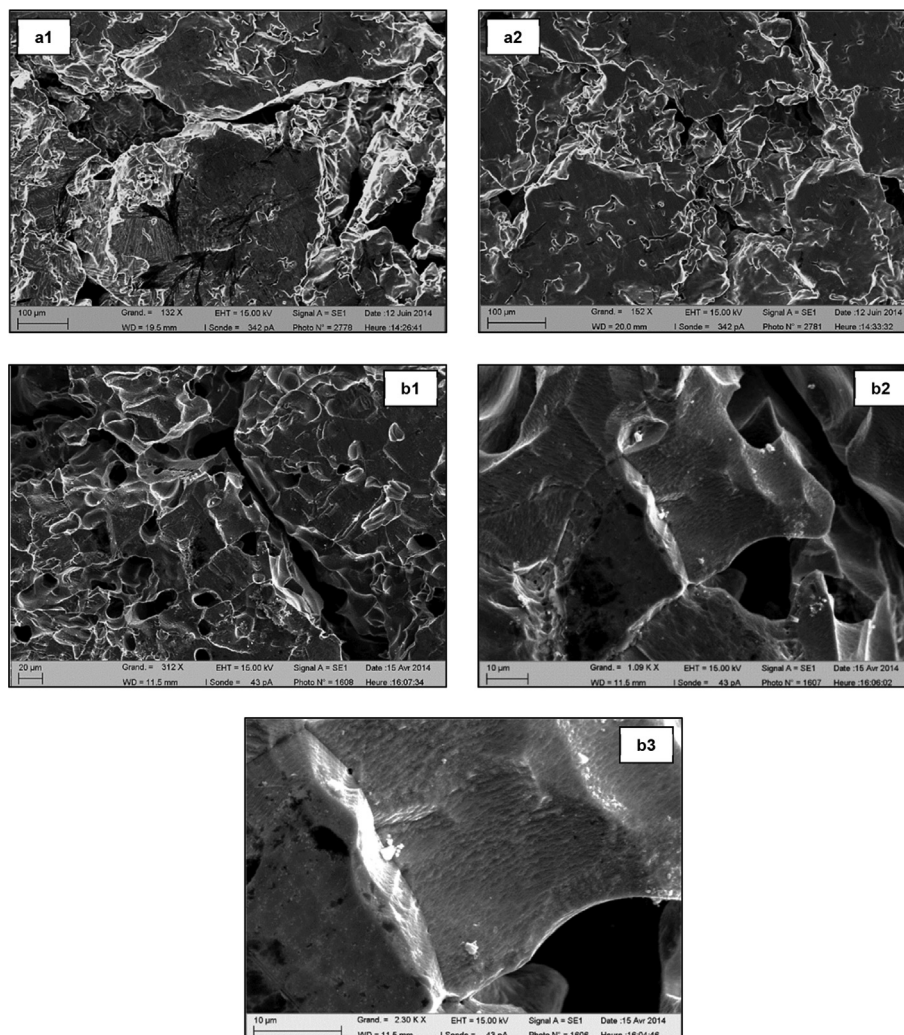
Fig. 8 – **SEM micrographs of the central zone (a) and of areas at the edge (b) of grade 2 titanium electrodes of the stacks after 5000 h of operation.**

[46,47]. In this case, the circulation of the electrolyte, with a flow rate of 6 m³/h, intervenes on the adhesion of the films and deposits and on the morphology of the surfaces. It facilitates the dissolution of the protective oxide film, which is less resistant in a strongly reducing medium (H_2SO_4 1 M), by creating an inhomogeneity of attack when the electrolyzer is in operation. The SEM observations make it possible to verify that the edge of the electrodes has indeed a more accentuated relief than the central area described above. This phenomenon is accentuated by the fact that the edge of the electrodes is directly in contact with the electrolyte since this zone is not coated (Fig. 8b1). Finally, the SEM micrographs carried out with a higher magnification (1000–2500 x) confirm this mechanism: they allow to observe the details of the grain and to highlight the corrosion in certain crystallographic planes as well as the presence of relatively large cavities on the grain surface (Fig. 8b2 and 8b3).

On the other hand, it is important to note that no intergranular rupture, as was the case for the tank, was observed on the electrodes. It is therefore possible to affirm that the

corrosion of titanium is here mainly due to the aggressiveness of sulfuric acid (1 M) [48], to the temperature (between 30 and 50 °C), to the mechanical and catalytic stresses generated by the circulation of the electrolyte, and not to embrittlement by hydrogen. Finally, the current flowing through the electrodes (0.3 A/cm²) also tends to accelerate the dissolution of titanium.

Characterization of hydrogen embrittlement

Glow Discharge Optical Emission Spectrometry (GDOES) was used to characterize the possible embrittlement of the degraded parts by hydrogen and to determine the diffusion depth of hydrogen on the surface after 5000 h of operation of the electrolyzer.

In order to carry out these investigations, a non-corroded grade 2 titanium plate was analysed to establish a reference profile (Fig. 9). This qualitative profile indicates the presence of carbon (grey curve), hydrogen (green curve) and oxygen (pink curve) on the surface of titanium (blue curve), due to pollution,
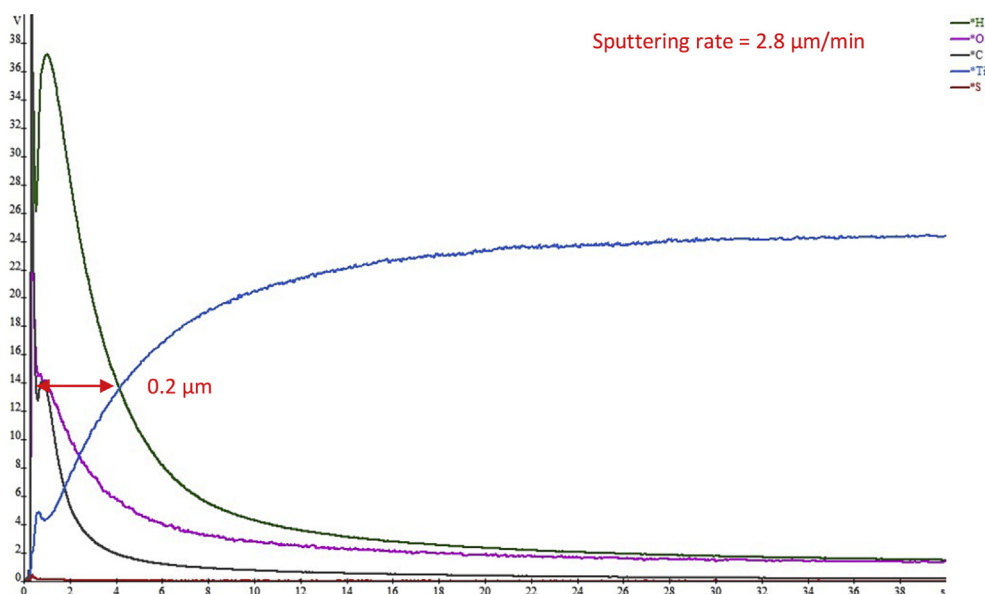
Sputtering rate = 2.8 μm/min

0.2 μm

Fig. 9 — **Qualitative reference depth profile of a grade 2 titanium non-corroded plate.**

oxidation and hydration of the non-corroded plate. Indeed, the more the analysis time increases, corresponding to the depth eroded by the argon plasma and characterized by the x-axis, the more the content, characterized by the y-axis, of hydrogen, oxygen and carbon, decreases while that of titanium increases. Therefore, after determining the sputtering rate (*cf. Material and methods*), it is possible to say that only a thin hydrated layer in extreme surface, 0.2 μm thick, contains hydrogen.

With the same method, the underside of the tank lid, strongly degraded, was analysed too. The profile obtained reveals the significant presence of hydrogen up to a great diffusion depth of about 12 μm, given the high roughness of the surface of the analysed part, due to the corrosion (Fig. 10). With the increase in hydrogen content, the surface structure of the film transforms from compact to porous, and the surface constituents from titanium oxides to titanium hydrides. Thus, it can be deduced that the electrochemical characteristics of the parts are affected because the corrosion resistance of the titanium is closely related to the structure and composition of the surface film exposed to the corrosive media [49–51]. This result tends to confirm the absorption of hydrogen having caused the degradation observed by SEM: intergranular fracture due to embrittlement at grain boundaries of the grade 2 titanium surface. However, since the corroded depth is much higher (192 μm on average according to measurements previously carried out by SEM), the embrittlement of titanium by hydrogen is not the only phenomenon responsible for the observed degradations.

Finally the degraded areas of the electrodes of the stacks were also characterized by GDOES (Fig. 11). The presence of carbon, hydrogen and oxygen is always observable. However, hydrogen is present to a slightly greater depth (0.5 μm) than for the non-corroded grade 2 titanium plate (0.2 μm). These results make it possible to confirm that the corrosion of the electrodes is not due to the diffusion of hydrogen in the

titanium and thus following an embrittlement. The damage observed on these parts is the consequence of the aggressiveness of the electrolyte (H_2SO_4 1 M), the parameters of use of the electrolyser (temperature, current) and mechanical phenomena (circulation of the electrolyte), causing the destruction of the protective passive film and the attack of titanium in uncoated areas, as has been interpreted from the characterizations performed by SEM [52].

Corrosion behaviour

The open-circuit potential (OCP) measurements and the potentiodynamic polarization curves to determine the corrosion current (i_{corr}) by Tafel slopes were performed in sulfuric acid medium (H_2SO_4 1 M) at room temperature.

Firstly, the observation of the OCP curves shows that the behaviour of the grade 2 titanium samples is reproducible from one test to another (Fig. 12). The analysis reveals that the titanium is in the passive state at first, its potential, characterized by the y-axis, around − 400 mV/SCE, does not evolve. The samples, left in the open air before the curves were drawn, covered with a thin film of titanium oxide which protects them from an attack of the immersion medium. This passive layer thus isolates the surface of the titanium from sulfuric acid. However after several hours of immersion (between 100 and 400 min), characterized by the x-axis, titanium becomes less and less noble: its potential decreases because its surface is attacked by the electrolyte. The protective oxide film is less efficient and titanium thus passes into solution in Ti^{3+} ion form. Then, the E_{OCP} stabilizes again fairly quickly at a value of − 675 mV/SCE. The corrodibility of titanium is then higher but a balance is created at the metal/solution (titanium/H_2SO_4) interface. The surface of the titanium is no longer totally passive: the protective oxide film, composed of corrosion products of titanium, oxides and/or titanium hydroxides, is formed continuously on the metal side but is
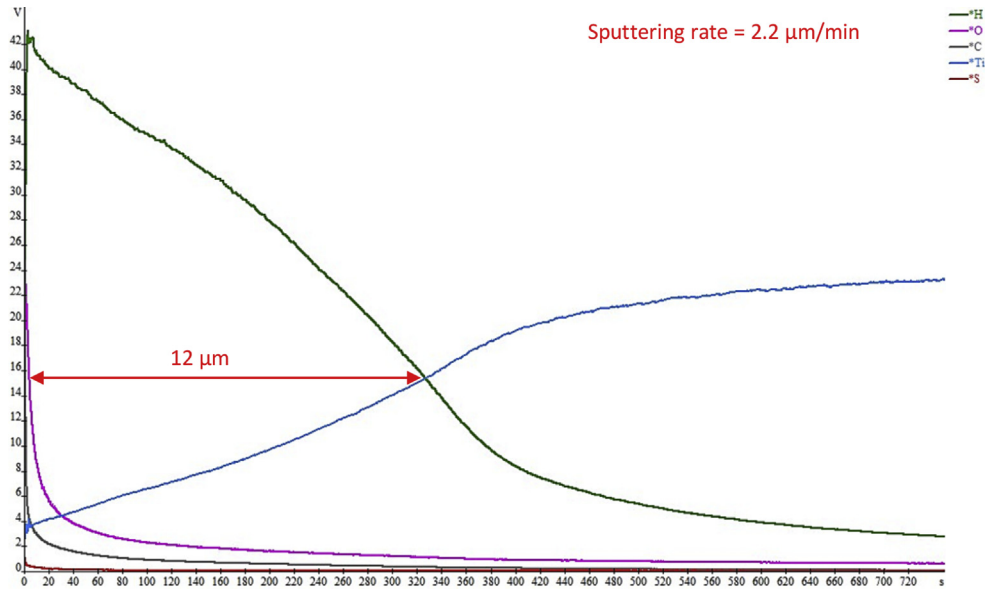
Fig. 10 — Qualitative depth profile of a degraded area of the grade 2 titanium hydrogen/H$_2$SO$_4$ separator (underside of the tank lid) after 5000 h of operation.

destroyed at the same time on the side of the solution, particularly aggressive (H$_2$SO$_4$ 1 M) [47]. The dissolution of grade 2 titanium, relatively slow, is then controlled by this equilibrium at the metal/solution interface. The E_{OCP}, of -675 mV/SCE, no longer evolves until the end of the analyses (24 h duration) (Fig. 12).

In a second step, the evolution of current density versus potential was analysed using polarization curves. And again, the behaviour of grade 2 titanium samples is well reproducible (Fig. 13). It should be noted that the value of the detected corrosion potential, about -250 mV/SCE, characterized by the x-axis, may vary depending on the initial surface condition of

the samples. This is the corrosion potential of grade 2 titanium in the passive state, without preparation, and therefore having a passive oxide film on its surface. In the case of a mechanically polished or pickled sample, the value would be of the order of -450 mV/SCE. By following the evolution of current density, characterized by the y-axis, from low potentials to high potentials, it is possible to observe, after switching to E_{OCP}, that the current density continues to increase slightly until the end of the test (Fig. 13). Titanium dissolves continuously in the sulfuric acid solution according to the reaction (7):
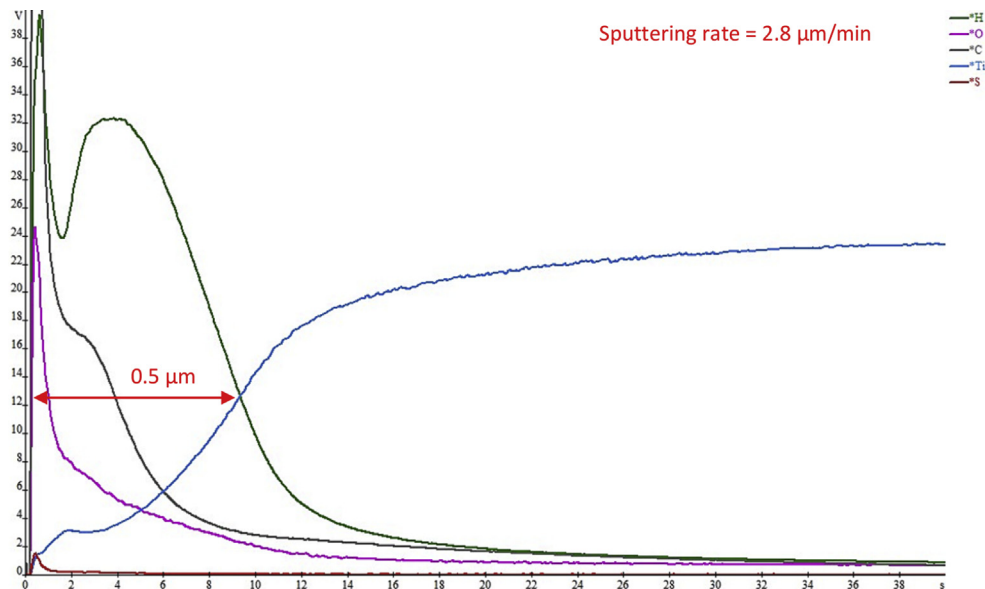
$$Ti \rightarrow Ti^{3+} + 3\ e^- \tag{7}$$

Fig. 11 — Qualitative depth profile of grade 2 titanium electrodes of the stacks after 5000 h of operation.
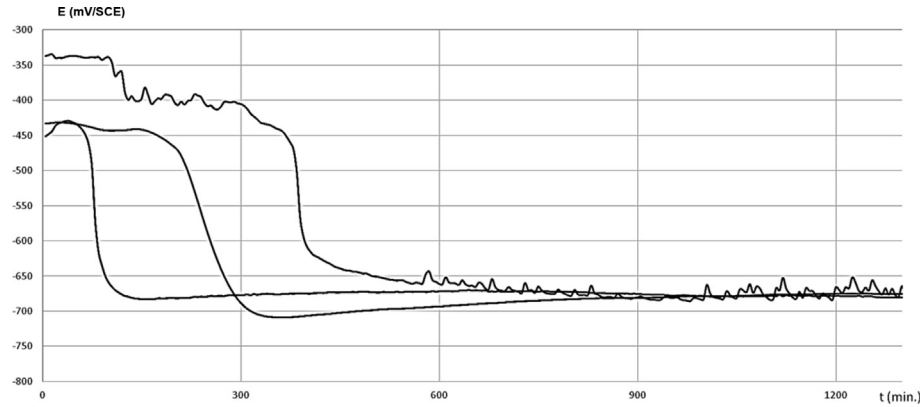
Fig. 12 — (E_{OCP}-t) curves of grade 2 titanium samples in sulfuric acid medium (H2SO4 1 M) at room temperature.
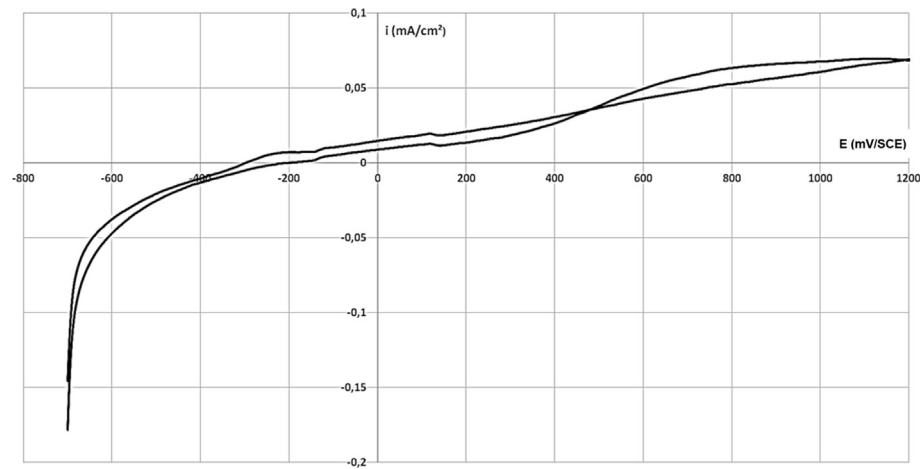

Fig. 13 — Polarization curves of grade 2 titanium samples in sulfuric acid medium (H_2SO_4 1 M) at room temperature.

The absence of a significant corrosion peak on the curves, added to the fact that the current density increases only slowly (from i_{corr} to 0.07 mA/cm^2), shows that the corrosion of the titanium is relatively slow. On the other hand, despite a certain equilibrium at the metal/solution interface slowing titanium dissolution, the absence of a passivation plateau shows that corrosion, even slow, is not negligible (Fig. 13). Indeed, the continuous formation of the protective oxide film on the surface of grade 2 titanium slows down its corrosion but, given the aggressiveness of the electrolyte, does not make it possible to suppress it.
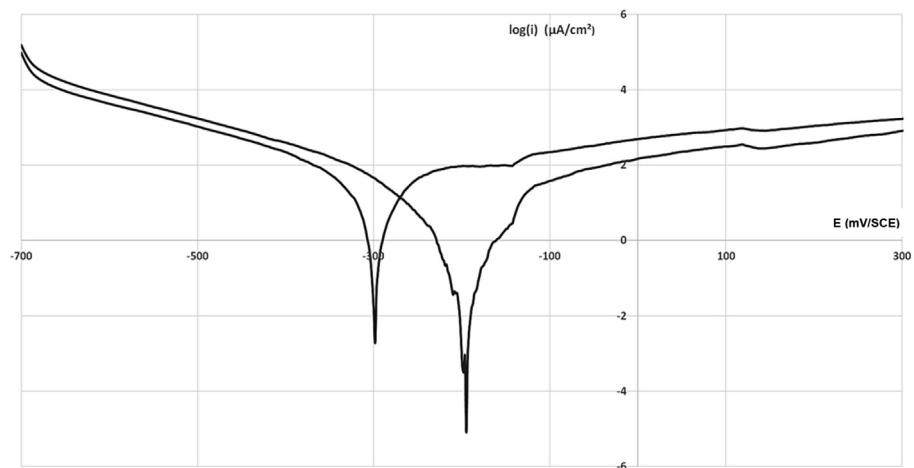

Fig. 14 — Tafel curves of grade 2 titanium samples in sulfuric acid medium (H_2SO_4 1 M) at room temperature.

Finally, in order to determine the grade 2 titanium corrosion current in the electrolyte (H_2O_4 1 M) by Tafel slopes, the corresponding curves were plotted (Fig. 14). The corrosion current density thus measured is of the order of 1.7 μA/cm^2 (average of all tests performed). And its average corrosion rate, under the same conditions, may therefore, by applying Faraday's law (equation (6)), estimated to be 20 μm/year, which seems very reasonable given the aggressiveness of the electrolyte. The actual conditions of use of the electrolyzers for the production of hydrogen are, however, slightly more severe, particularly in temperature (between 30 and 50 °C), pressure (up to 16 bar) and current (of 0.3 A/dm^2 running through the electrolyte), than the chosen parameters during the tests carried out in the laboratory. Therefore, the corrosion rate of the grade 2 titanium of the electrodes in operation is most certainly slightly higher than the estimated corrosion rate.

Conclusions

This study allowed, after characterization by Scanning Electron Microscopy and Glow Discharge Spectrometry of the observed deteriorations on the different grade 2 titanium parts used in the electrolyzers for hydrogen production, to determine the corrosion mechanisms for each type of part. It has thus been possible to demonstrate that the electrodes of the stacks corrode, given the aggressiveness of the medium and the operating parameters of the electrolyzers, according to a fairly conventional generalized corrosion (destruction of the passive oxide film, accelerated by the circulation of the electrolyte, and dissolution of titanium by sulfuric acid). With regard to the hydrogen/H_2SO_4 separator, a significant diffusion of hydrogen in titanium (up to a depth greater than 12 μm) has been characterized by GDOES, the SEM analysis revealing in turn an intergranular fracture on the surface, the embrittlement of titanium with hydrogen could be demonstrated.

In a second step, the electrochemical methods of corrosion analysis made it possible to verify that the choice of grade 2 titanium was justified for the design of the electrodes of the stacks. Its free potential in a sulfuric medium tends to stabilize over time and its corrosion rate, probably slightly greater than 20 μm/year under the actual operating conditions of the electrolyzers, is acceptable.

Therefore, in the context of use in the manufacture of electrolyzers for hydrogen production, it would be interesting to test corrosion behaviour of certain grades of stainless steels in the same conditions, for use in the design of the hydrogen/H_2SO_4 separator instead of titanium. And as regards the various titanium stacks parts, an electrochemical study carried out in sulfuric medium in the presence of inhibitors could demonstrate that it is possible to improve the corrosion resistance of titanium in the electrolyte.

These two points will be the subject of a future study.

Data availability

The raw/processed data required to reproduce these findings cannot be shared at this time as the data also forms part of an ongoing study.

REFERENCES

[1] Gahleitner G. Hydrogen from renewable electricity: an international review of power-to-gas pilot plants for stationary applications. Int J Hydrogen Energy 2013;38:2039–61.

[2] Chu S, Majumdar A. Opportunities and challenges for a sustainable energy future. Nature 2012;488:294–303.

[3] Zou X, Zhang Y. Noble metal-free hydrogen evolution catalysts for water splitting. Chem Soc Rev 2015;44:5148–80.

[4] Seh ZW, Kibsgaard J, Dickens CF, Chorkendorff I, Norskov JK, Jaramillo TF. Combining theory and experiment in electrocatalysis: insights into materials design. Science 2017;355.

[5] Staszak-Jirkovsky J, Malliakas CD, Lopes PP, Danilovic N, Kota SS, Chang KC, et al. Design of active and stable Co-Mo-Sx chalcogels as pH-universal catalysts for the hydrogen evolution reaction. Nat Mater 2016;15:197–203.

[6] Zhang Y, Ouyang B, Xu J, Chen S, Rawat RS, Fan HJ. 3D porous hierarchical nickel-molybdenum nitrides synthesized by RF plasma as highly active and stable hydrogen-evolution reaction electrocatalysts. Ad Energy Mater 2016;6:16002–21.

[7] Jamesh MI. Recent progress on earth abundant hydrogen evolution reaction and oxygen evolution reaction bifunctional electrocatalyst for overall water splitting in alkaline media. J Power Sources 2016;333:213–36.

[8] Bodineau L, Mussot J-L, Verbecke F, Mofakhami A. Guide d'information sur les risques et les mesures de sécurité liés à la production décentralisée d'hydrogène. INERIS et ENEA Consulting. Guide d'information ADEME; 2015.

[9] Li Y, Wang H, Wang R, He B, Gong Y. 3D self-supported Fe-O-P film on nickel foam as a highly active bifunctional electrocatalyst for urea-assisted overall water splitting. Mater Res Bull 2018;100:72–5.

[10] Ma Z, Zhao Q, Li J, Tang B, Zhang Z, Wang X. Three-dimensional well-mixed/highly-densed NiS-CoS nanorod arrays: an efficient and stable bifunctional electrocatalyst for hydrogen and oxygen evolution reactions. Electrochim Acta 2018;260:82–91.

[11] Wu Z, Zou Z, Huang J, Gao F. Fe-doped NiO mesoporous nanosheets array for highly efficient overall water splitting. J Catal 2018;358:243–52.

[12] Bertuccioli L, Chan A, Hart D, Lehner F, Madden B, Standen E. Study on development of water electrolysis in the EU. Fuel cells and hydrogen Joint undertaking. Final Report; 2014.

[13] Pura JA, Bobyn JD, Tanzer M. Implant-delivered alendronate causes a dosedependent response on net bone formation around porous titanium implants in canines. Clin Orthop Relat Res 2016;474:1224–33.

[14] Everaerts J, Gontcharov D, Verlinden B, Wevers M. The influence of load holds on the fatigue behaviour of drawn Ti-6Al-4V wires. Int J Fatigue 2017;98:203–11.

[15] Simcoe CR. Titanium: a metal for the aerospace age – part I. Adv Mater Process 2015;173(3):30–1.

[16] Harada R, Takemoto S, Kinoshita H, Yoshinari M, Kawada E. Influence of sulfide concentration on the corrosion behavior of titanium in a simulated oral environment. Mater Sci Eng C 2016;62:268–73.

[17] Diamanti MV, Souier T, Stefancich M, Chiesa M, Pedeferri MP. Probing anodic oxidation kinetics and nanoscale heterogeneity within TiO2 films by Conductive Atomic Force Microscopy and combined techniques. Electrochim Acta 2014;129:203–10.

[18] Lu JQ, Wei GY, Yu YD, Zhao XP, Dai YF. Enhanced corrosion resistance of TA2 titanium via anodic oxidation in mixed acid system. Int. J. Electrochem. Sci. 2017;12:2763–76.

[19] Carmo M, Fritz DL, Mergel J, Stolten D. A comprehensive review on PEM water electrolysis. Int J Hydrogen Energy 2013;38:4901—34.

[20] Singh AK, Rarotra S, Pasumarthi V, Mandalab TK, Bandyopadhyay D. Formic acid powered reusable autonomous ferrobots for efficient hydrogen generation under ambient conditions. J Mater Chem 2018;6:9209—19.

[21] Ito H, Kawaguchi N, Someya S, Munakata T, Miyazaki N, Ishida M, Nakano A. Experimental investigation of electrolytic solution for anion exchange membrane water electrolysis. Int J Hydrogen Energy 2018;43:1703—17039.

[22] Giddey Sarbjit, Badwal Sukhvinder PS, Ju HyungKuk. Polymer electrolyte membrane technologies integrated with renewable energy for hydrogen production. Curr Trends Future Dev (Bio-) Membr 2019:235—59.

[23] Budak Yağmur, Devrim Yılser. Comparative study of PV/PEM fuel cell hybrid energy system based on methanol and water electrolysis. Energy Convers Manag 2019;179:46—57.

[24] Moradi Nafchi F, Baniasadi E, Afshari E, Javani N. Performance assessment of a solar hydrogen and electricity production plant using high temperature PEM electrolyzer and energy storage. Int J Hydrogen Energy 2018;43:5820—31.

[25] Christian Olesen A, Henrik Frensch S, Knudsen Kær S. Towards uniformly distributed heat, mass and charge: a flow field design study for high pressure and high current density operation of PEM electrolysis cells. Electrochim Acta 2019;293:476—95.

[26] Carrere P, Prat M. Liquid water in cathode gas diffusion layers of PEM fuel cells: identification of various pore filling regimes from pore network simulations. Int J Heat Mass Transf 2019;129:1043—56.

[27] Xing Lei, Xu Yuanxiang, Das Prodip K, Maoc Baodong, Xu Qian, Su Huaneng, XuWue, Shi Weidong. Numerical matching of anisotropic transport processes in porous electrodes of proton exchange membrane fuel cells. Chem Eng Sci 2019;195:127—40.

[28] Peters M, Hemptenmacher J, Kumpfert J, Leyens C. Structure and properties of titanium and titanium alloys. In: Titanium and titanium alloys: fundamentals and applications chap. 1. Wiley-VCH; 2003. p. 1—36.

[29] Liu ZJ, Zhong X, Walton J, Thompson GE. Anodic film growth of titanium oxide using the 3-electrode electrochemical technique: effects of oxygen evolution and morphological characterizations. J Electrochem Soc 2016;163(3):E75—82.

[30] Li XF, Chen NN, Chen J, Mei QF, Wan L, Jia CL, Liu H. Superplastic deformation behavior of Ti-55 alloy without and with 0.1 wt% H addition. Mater Sci Eng 2017;704:386—90.

[31] Wu W, Liu ZY, Hu SS, Li XG, Du CW. Effect of pH and hydrogen on the stress corrosion cracking behavior of duplex stainless steel in marine atmosphere environment. Ocean Eng 2017;146:311—23.

[32] Liu ZY, Wang XZ, Du CW, Li JK, Li XG. Effect of hydrogen-induced plasticity on the stress corrosion cracking of X70 pipeline steel in simulated soil environments. Mater Sci Eng 2016;658:348—54.

[33] Liu Y, Xiang W, Zhang GL, Wang BY. Surface and phase transformation characteristics of titanium hydride film under irradiation of pulsed ion beam. Appl Surf Sci 2013;285P:557—63.

[34] Eliezer D, Tal-Gutelmacher E, Cross CE, Boellinghaus Th. Hydrogen absorption and desorption in a duplex-annealed Ti—6Al—4V alloy during exposure to different hydrogen-containing environments. Mater Sci Eng 2006;433:298—304.

[35] Nikiforov AV, Petrushina IM, Christensen E, Tomas-Garcia AL, Bjerrum NJ. Corrosion behaviour of construction materials for high temperature steam electrolysers. Int J Hydrogen Energy 2011;36:111—9.

[36] Payling R, Jones D, Bengtson A. Glow discharge optical emission Spectrometry. Chichester: J. Wiley & Sons; 1997.

[37] Nelis T, Payling R. Glow discharge optical emission spectroscopy: a practical guide. Cambridge: RSC Analytical Spectroscopy Monographs; 2003.

[38] Marcus K. Glow discharge spectroscopies. Plenum Publishing Corporation; 1993.

[39] Wang K, Pickering HW, Weill KG. Electrochem. Acta 2001;46:3835.

[40] Lin K-L, Liu T-P. Mater Chem Phys 1998;56:171.

[41] Veeraraghavan B, haran B, Kumaraguru SP, Popov BN. J Electrochem Soc 2003;150:B131.

[42] de Assis SL, Wolynec S, Costa I. Corrosion characterization of titanium alloys by electrochemical techniques. Electrochim Acta 2006;51:1815—9.

[43] Dubent S, Mertens MLAD, Saurat M. Electrodeposition, characterization and corrosion behaviour of tin—20 wt.% zinc coatings electroplated from a non-cyanide alkaline bath. Mater Chem Phys 2010;120:371—80.

[44] Sheit DS, Robertson IM, Birnraum HK. Hydrogen embrittlement of α titanium: in situ TEM studies. Acta Metall 1988;36:111—24.

[45] Cecile B, Ollivier P, Bloise R, Kauffmann JP. J Less Common Met 1980;70:39—58.

[46] Wilhelmsen W, Grande AP. The influence of hydrofluoric-acid and fluoride-ion on the corrosion and passive behavior of titanium. Electrochim Acta 1987;32:1469—74.

[47] Pouilleau J, Devilliers D, Garrido F, Durand-Vidal S, Mah E. Structure and composition of passive titanium oxide films. Mater Sci Eng 1997;B47:235—43.

[48] Richardson JA. Corrosion in sulfuric acid. Shreir's Corrosion 2010;2:1226—49.

[49] Wu Wei, Liu Jing, Liu Zhiyong, Cui Liying, Du Cuiwei, Li Xiaogang. Surface characterization of the commercially pure titanium after hydrogen charging and its electrochemical characteristics in artificial seawater. J Electroanal Chem 2018;822:23—32.

[50] Wang ZB, Hu HX, Zheng YG. Evaluation of the dissolved oxygen-related electrochemical behavior of pure titanium in acidic fluoride-containing solutions. J Solid State Electrochem 2016;(12):3459—71.

[51] Hao WK, Liu ZY, Wu W, Li XG, Du CW, Zhang DW. Electrochemical characterization and stress corrosion cracking of E690 high strength steel in wet-dry cyclic marine environments. Mater Sci Eng 2018;710:318—28.

[52] Utomo WB, Donne SW. Electrochemical behaviour of titanium in H2SO4—MnSO4 electrolytes. Electrochim Acta 2006;51:3338—45.